Dynamics of modal power distribution in a multimode semiconductor laser with optical feedback

J.M. Buldú, J. Trull, M.C. Torrent, J. García-Ojalvo

Departament de Física i Enginyeria Nuclear, Universitat Politècnica de Catalunya, Colom 11, E-08222 Terrassa, Spain

Claudio R. Mirasso

Departament de Física, Universitat de les Illes Balears, E-07071 Palma de Mallorca, Spain

The dynamics of power distribution between longitudinal modes of a multimode semiconductor laser subjected to external optical feedback is experimentally analyzed in the low-frequency fluctuation regime. Power dropouts in the total light intensity are invariably accompanied by sudden activations of several longitudinal modes. These activations are seen not to be simultaneous to the dropouts, but to occur after them. The phenomenon is statistically analysed in a systematic way, and the corresponding delay is estimated.

OCIS codes: 140.1540, 140.5960

Semiconductor lasers are devices very susceptible to exhibiting unstable dynamical behavior. When subjected to reflections of its own emitted radiation, in particular, they easily enter complex dynamical regimes, exhibiting for instance low-frequency fluctuations (LFF) in the form of intensity dropouts[1], or fully-developed chaotic fluctuations leading to coherence collapse[2]. Most of the related theoretical and experimental studies undertaken so far have dealt with the dynamics of the total emitted intensity[3,4]. However, the low-cost semiconductor lasers employed in technological applications operate usually in several longitudinal modes. Therefore, analysing the mode dynamics would be necessary, a need which has been recognized only recently[5]. In particular, recent experiments have indeed shown the importance of multimode operation in the LFF regime[6,7]. Different dynamical[8,9] and statistical[10] characteristics of this regime have been described in terms of a multimode extension of the well-known Lang-Kobayashi model[11].

In the course of the above-mentioned investigations, it was observed that when the feedback was frequency-selective (such as that provided by a diffraction grating), the intensity dropouts were accompanied by a sudden activation of other longitudinal modes of the laser[6,12]. These modes, located at the sides of the main mode in the gain curve, will be called longitudinal side modes, or simply side modes, in the rest of this Letter. The activation of these modes was heuristically interpreted as the mechanism producing the intensity dropouts[12], and was numerically reproduced again by a multimode LK model[13]. In this Letter, we show experimentally that the side-mode activation also appears in the presence of non-frequency-selective feedback, and that it occurs neither simultaneously nor previously to the intensity dropout,

but *after* it. Therefore, in this case this activation can not be the cause, but rather the effect, of the dropout.

Our experimental setup is shown schematically in Fig. 1. We use an index-guided single-transverse-mode AlGaInP semiconductor laser (Roithner RLT6505G), emitting at a nominal wavelength of 650 nm with a threshold current of 20.1 mA. Its temperature is set to 24.00 ± 0.01 °C. The laser output is collimated by an antireflection-coated laser-diode objective. An external mirror is placed 60 cm away from the front facet of the solitary laser, which corresponds to a feedback time of 4 ns. The threshold reduction due to the feedback is 9.4%. Throughout the paper, the injection current is set to 1.09 times the solitary laser threshold.
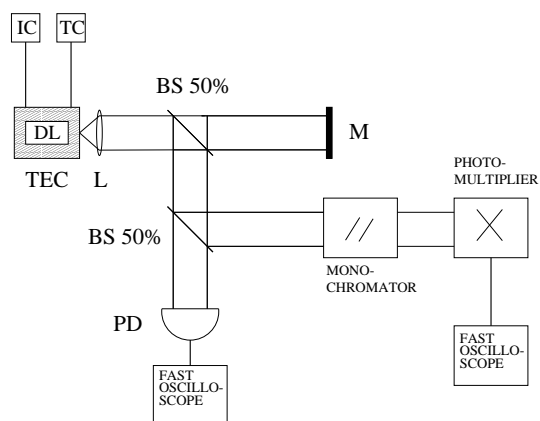

Fig. 1. Experimental setup: LD, laser diode; BS, beam splitter; M, external mirror; TEC, laser diode mount; PD, photodiode; IC, intensity controller; TC, temperature controller.

Part of the total output intensity is detected by

1

a fast photodiode and sent to a 500 MHz-bandwidth HP 54720D digital oscilloscope. The rest passes through a $1/8m$ CVI monochromator with a resolution better than 0.2 nm, used to select the laser modes, and whose output is sent to a Hamamatsu PS325 photomultiplier. The photomultiplier signal is also recorded by the oscilloscope.

The optical spectrum of our solitary laser shows at least ten active longitudinal modes, with its maximum located at $\sim$658.4 nm and a FWHM of $\sim$0.9 nm. When the feedback is turned on, the spectrum broadens (up to a FWHM of $\sim$1.3 nm), and its maximum becomes shifted $\sim$0.5 nm towards higher wavelengths[4,14]. For the feedback parameters chosen, mentioned above, the laser emits in the low-frequency fluctuation regime. In this regime, we have compared the dynamical behavior of the total emitted intensity of the laser with that of the main mode of the laser with feedback (MMF), and with a longitudinal side mode corresponding to the original main mode of the solitary laser (MMS). The typical behavior is displayed in Fig. 2, which compares the total intensity evolution with either that of the MMF (traces a-b) or the MMS (traces c-d). It can be seen that a power dropout is associated to an abrupt decay of the former and a sudden activation of the latter. Note that the recovery of the MMF is much slower than that of the total intensity, a fact that has been already reported in the literature[6,15]. The activation is seen not to be symmetric, i.e. it does not occur in the other side of the spectrum. We have found similar behavior in other semiconductor lasers of similar quality, including nearly-single-mode lasers.
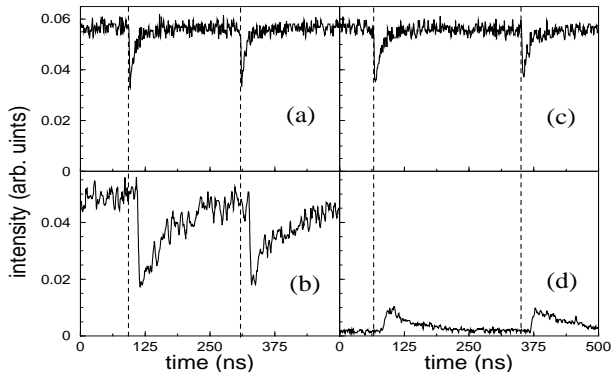

Fig. 2.   Modal structure of a dropout. Total intensity evolution (a,c) compared to that of the main mode of the laser with feedback (b) and of the original main mode of the solitary laser (d). Traces (a,b) and (c,d) have been acquired simultaneously (but note the intrinsic delay of the mode-selecting path of the setup – see text). Vertical dashed lines are a guide to the eye.

We note that, even though the pairs of measurements (a,b) and (c,d) in Fig. 2 were acquired simultaneously, the time traces exhibit a systematic delay of $\sim$20 ns between the total-intensity dropouts and the corresponding modal powers (see vertical dashed lines in the figure). This delay is spurious, due to the electronic response time of the photomultiplier used in the mode-selecting path of the experimental setup (Fig. 1), which is substantially larger than that of the photodiode used to measure the total intensity. However, as we will show in what follows, a closer inspection of these results reveals that this spurious delay is slightly *larger* for the MMS activation than for the MMF dropout. Since both of these signals are measured with the same detector, this observation leads to the conclusion that the side-mode activation does not occur simultaneously to (nor before) the dropout, but *after* it.

In order to estimate the delay between each dropout and its MMS activation we proceed as follows. First, several (typically 40) time-trace pairs containing a single total-intensity dropout and its simultaneously measured modal event (either MMF dropout or MMS activation) are averaged using a predefined event (a given decay of the total intensity in our case) as a trigger. In this way, we average out fluctuations before the dropout event and during the subsequent build-up, and refer all the time traces to a common time origin (given by the predefined event mentioned above). The result of this procedure is shown in Fig. 3(a). One can already see in this figure, which shows several averaged sets for each one of the three quantities measured (total intensity, MMF intensity, and MMS intensity), that the MMS activation occurs somewhat later ($\sim$1 ns) than the MMF dropout (see vertical dashed lines in the figure). In order to identify such a delay more clearly, we compare in Fig. 3(b) the MMS signal to the inverted MMF one. The delay becomes now evident. Note also that the escape trajectories of the two modes (from the lasing state in the MMF case, and from the off state in the MMS case) are basically parallel, which indicates that the instability mechanisms are the same, and hence a direct comparison between them can be made.

We estimate the delay between the dropout and the side-mode activation as the distance between the two corresponding parallel escaping trajectories, which can be clearly identified in Fig. 3(b) as two distinct sets of straigh lines with the same positive slope. We perform a piecewise local linear fit of each one of the averaged MMF and MMS time series, and identify the time instants at which the slope takes its maximum value. Figure 4 represents the distribution of these times, for both the MMS activation and the MMF dropout, computed from an statistics of 3000 dropout events. The distribution functions of these two quantities are clearly sep-

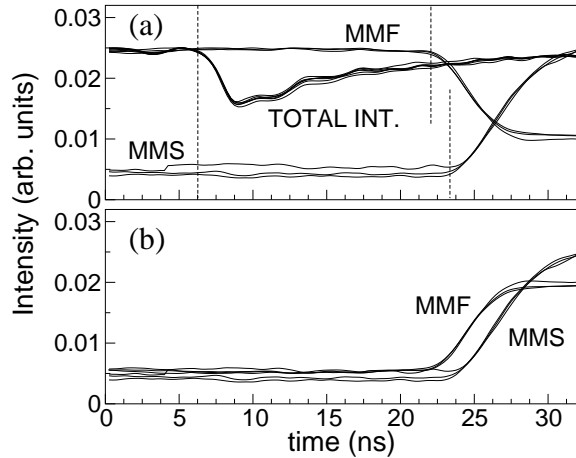arated, with a time difference between their two mean values of 1.5±1.1 ns.

Fig. 3. Averaged time traces of a dropout in the total intensity, main mode of the laser with feedback, and main mode of the solitary laser. In plot (b), the traces of the MMF have been inverted.
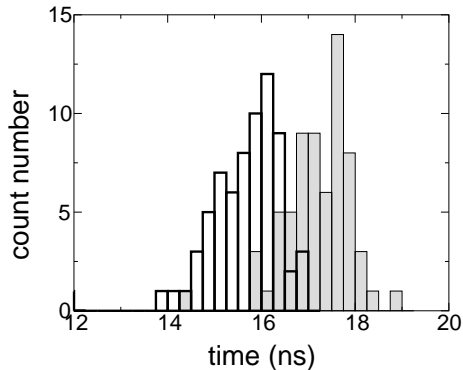

Fig. 4. Distribution of times of occurrence of both the dropouts of the main mode of the laser with feedback (white bars) and the activations of the side mode – main mode of the solitary laser (grey bars).

In conclusion, we have experimentally shown that low-frequency fluctuations in a multimode semiconductor laser with global (i.e. non-frequency selective) optical feedback are associated to sudden activations of a longitudinal side mode corresponding to the main mode of the solitary laser. These activations are seen to occur after the dropouts of the main mode of the laser with feedback, and hence after the total intensity dropouts of the system. Therefore, in this case the side-mode activation cannot account for the destabilization giving rise to the low-frequency fluctuations. On the contrary, one can conjecture that the activations are a natural consequence of the loss of power in the main modes of the laser with feedback. Work directed to the theoretical modeling of these phenomena is in progress[14].

1. Ch. Risch and C. Voumard, J. Appl. Phys. **48**, 2083 (1977).
2. D. Lenstra, B. Verbeek, and A.J. de Boef, IEEE J. Quantum Electron. **21**, 764 (1985).
3. J. Mork, J. Mark, B. Tromborg, Phys. Rev. Lett. **65**, 1999 (1990); T. Sano, Phys. Rev. A **50**, 2719 (1994); A. Hohl, H.J.C. van der Linden, and R. Roy, Opt. Lett. **20**, 2396 (1995); I. Fischer, G.H.M. van Tartwijk, A.M. Levine, W. Elsäßer, E. Göbel, and D. Lenstra, Phys. Rev. Lett. **76**, 220 (1996); C. Masoller and N.B. Abraham, Phys. Rev. A **57**, 1313 (1998); J. Mulet and C.R. Mirasso, Phys. Rev. E **59**, 5400 (1999).
4. T. Heil, I. Fischer, W. Elsäßer, J. Mulet, and C.R. Mirasso, Opt. Lett. **24**, 1275 (1999).
5. A.T. Ryan, G.P. Agrawal, G. R. Gray, and E. C. Gage, IEEE J. Quantum Elec. **30**, 668 (1994).
6. G. Huyet, S. Balle, M. Giudici, C. Green, G. Giacomelli, and J. R. Tredicce, Opt. Comm. **149**, 341 (1998).
7. G. Vaschenko, M. Giudici, J.J. Rocca, C.S. Menoni, J.R. Tredicce, and S. Balle, Phys. Rev. Lett. **81**, 5536 (1998).
8. E.A. Viktorov and P. Mandel, Phys. Rev. Lett. **85**, 3157 (2000); T.W. Carr, D. Pieroux, and P. Mandel, Phys. Rev. A **63**, 033817 (2001).
9. F. Rogister, P. Mégret, O. Deparis and M. Blondel, Phys. Rev. A **62**, 061803(R) (2001).
10. D.W. Sukow, T. Heil, I. Fischer, A. Gavrielides, A. Hohl-AbiChedid, and W. Elsäßer, Phys. Rev. A **60**, 667 (1999).
11. R. Lang and K. Kobayashi, IEEE J. Quantum Electron. **16**, 347 (1980).
12. M. Giudici, L. Giuggioli, C. Green, and J.R. Tredicce, Chaos, Solitons and Fractals **10**, 811 (1999).
13. E.A. Viktorov and P. Mandel, Opt. Lett. **25**, 1576 (2000).
14. J.M. Buldú, F. Rogister, J. Trull, M.C. Torrent, J. García-Ojalvo, and C.R. Mirasso, in preparation (2001).
15. I. Wallace, D. Yu, R. G. Harrison and A. Gavrielides, J. Opt. B, **2**, 447, (2000).